THE JOURNAL OF BIOLOGICAL CHEMISTRY
Vol. 273, No. 39, Issue of September 25, pp. 25427–25435, 1998

Printed in U.S.A.

IκBα Functions through Direct Contacts with the Nuclear Localization Signals and the DNA Binding Sequences of NF-κB*

(Received for publication, May 29, 1998, and in revised form, July 8, 1998)

Shiva Malek‡, Tom Huxford§, and Gourisankar Ghosh¶

From the Department of Chemistry and Biochemistry, University of California, San Diego, California 92093-0359

We have determined the binding energies of complexes formed between IκBα and the wild type and mutational variants of three different Rel/NF-κB dimers, namely, the p50/p65 heterodimer and homodimers of p50 and p65. We show that although a common mode of interaction exists between the Rel/NF-κB dimers and IκBα, IκBα binds the NF-κB p50/p65 heterodimer with 60- and 27-fold higher affinity than the p50 and p65 homodimers, respectively. Each of the three flexibly linked segments of the rel homology region of Rel/NF-κB proteins (the nuclear localization sequence, the dimerization domain, and the amino-terminal DNA binding domain) is directly engaged in forming the protein/protein interface with the ankyrin repeats and the carboxyl-terminal acidic tail/PEST sequence of IκBα. In the cell, IκBα functions to retain NF-κB in the cytoplasm and inhibit its DNA binding activity. These properties are a result of the direct involvement of the nuclear localization sequences and of the DNA binding region of NF-κB in complex with IκBα. A model of the interactions in the complex is proposed based on our observations and the crystal structures of Rel/NF-κB dimers and the ankyrin domains of related proteins.

The Rel/NF-κB family of dimeric transcription factors is ubiquitous in all human cell types. NF-κB regulates the expression of a variety of genes essential for cellular immune responses, inflammation, and growth and development (1–3). Transcriptionally active NF-κB dimers form through the combinatorial assembly of the five monomeric polypeptides, p50, p65, p52, c-Rel, and RelB. Each monomer shares an approximately 300-amino acid region known as the rel homology region (RHR).[1] Within the RHR of the NF-κB polypeptides are all of the amino acid residues required for subunit dimerization, specific DNA binding, and nuclear localization (2, 3). Crystallographic analyses of the p50RHR (4, 5) and the dimerization domain of p65 (p65ddNLS) (6) revealed that the 13 carboxyl-terminal amino acids containing the nuclear localization sequence (NLS) are not part of the dimerization domain of p50 and p65. The carboxyl-terminal NLS segments of p50 and p65 are not visible in the electron density maps and are presumably unstructured in solution. Subsequent crystal structures of the RHR dimers of p52 (7), p65 (8), and p50/p65 (9) used smaller RHR versions that exclude the carboxyl-terminal 13 amino acids. These structures display folds similar to p50RHR. Together, these structures indicate that the RHR of the NF-κB transcription factors is composed of three mutually independent modules. 1) An amino-terminal domain, composed of roughly 200 amino acids, assumes an immunoglobulin-like tertiary fold and is primarily responsible for conferring DNA binding specificity. 2) The central dimerization domain, approximately 100 amino acids in length, also exhibits an immunoglobulin fold. 3) The NLS, composed of 13 residues at the carboxyl terminus, appears to be flexible in solution (Fig. 1*A, top panel*).

The nuclear translocation and DNA binding activities of the NF-κB proteins are inhibited through association with a member of the IκB family of transcription factor inhibitors (3). A host of extracellular stimuli trigger various signal transduction cascades, which converge at the phosphorylation of IκBα or IκBβ in complex with a dimer of NF-κB (2, 10–12). The phosphorylated IκB proteins become targets for ubiquitination and subsequent proteosome-mediated degradation (13). Free NF-κB dimers can then readily translocate the nuclear envelope and bind to their specific DNA target sites. An analogous mechanism for activation of transcription exists in *Drosophila melanogaster* development. The morphogen regulatory transcription factor Dorsal exists in an inactive cytoplasmic complex with its inhibitor, Cactus. These two proteins are structurally and functionally related to the NF-κB and IκB proteins, respectively (14–16).

Members of the IκB family of proteins contain six to seven homologous copies of an approximately 33-amino acid sequence known as the ankyrin repeat (3). The three-dimensional structures of four different ankyrin repeat containing proteins (17–20) show that ankyrin repeats assume a unique structural scaffold in which a "finger-like" β-hairpin is projected from the core helix-turn-helix element. The ankyrin repeat domain of IκBα, consisting of six imperfect repeats, is preceded by a 70-amino acid amino-terminal segment and followed by a 42-amino acid carboxyl-terminal region (21) (Fig. 1*A, bottom panel*). The amino-terminal segment, referred to as the signal response domain (SRD), receives signals through the phosphorylation of serines at positions 32 and 36. The SRD is not known to play any role in NF-κB binding (11, 22, 23). The carboxyl-terminal segment is rich in proline, glutamic acid/aspartic acid, serine, and threonine residues (the PEST sequence). This PEST sequence is a common feature implicated in high turnover rate among short-lived proteins (24). Partial or complete deletion of the acidic PEST region reduces the ability of IκBα to inhibit DNA binding of certain NF-κB dimers (25–27). Other IκB family proteins also contain a similar do-

* This work was supported by a National Institutes of Health research grant (to G. G.). The costs of publication of this article were defrayed in part by the payment of page charges. This article must therefore be hereby marked "*advertisement*" in accordance with 18 U.S.C. Section 1734 solely to indicate this fact.

‡ Supported by a predoctoral training grant from the National Institutes of Health, National Research Service Award 2 T32 GM08326.

§ Supported by National Institutes of Health/National Cancer Institute training grant, National Research Service Award I32 CA09523-13.

¶ To whom correspondence should be addressed: Department of Chemistry and Biochemistry, University of California, San Diego, 9500 Gilman Dr., La Jolla, CA 92093-0359. Tel.: 619-822-0469; Fax: 619-534-6174; E-mail: gghosh@ucsd.edu.

[1] The abbreviations used are: RHR, rel homology region; NLS, nuclear localization sequence; SRD, signal response domain; GST, glutathione *S*-transferase.

main structure, with the notable exceptions of p105 and p110, which contain NF-κB p50 and p52 sequences, respectively, at their amino termini.

It is generally believed that the IκB proteins retain NF-κB in the cytoplasm by precluding the NLS of the NF-κB RHR from being recognized by the nuclear transport machinery (1, 2). In addition, studies have shown that one IκBα molecule interacts with one NF-κB dimer (25). However, it is not known whether the IκB proteins directly contact the NLS or mask it by steric hindrance (28, 29). Furthermore, it has not been determined whether one or both of the NF-κB NLSs are involved in this process. One other intriguing property of IκBα is that in the post-induction stage, newly synthesized IκBα can enter the nucleus, where it is capable of dissociating transcriptionally competent NF-κB/DNA complexes (30, 31). It remains to be seen whether this inhibition of DNA binding activity of IκBα occurs through interaction with the DNA binding residues of NF-κB. There exists no clear evidence as to why the NF-κB p50/p65 heterodimer is preferentially recognized by IκBα over the p50, p65, or c-Rel homodimers. Furthermore, the role of the p50 subunit of the p50/p65 heterodimer in its interaction with IκBα is not known. Finally, it remains unclear what role, if any, the amino-terminal DNA binding domain of the NF-κB RHR plays in the NF-κB/IκB complex.

Using fluorescence polarization competition experiments, we have determined the equilibrium dissociation constants of the complexes between NF-κB (wild type and mutant p50 and p65 homodimers and the p50/p65 heterodimer) and IκBα. We show that IκBα recognizes the NF-κB dimers with variable affinities. In binding to the heterodimer, IκBα directly contacts the NLSs of both subunits in addition to making contacts with the dimerization domains and the DNA binding loop L1 of the p65 subunit. We suggest that the mode of interaction between each of the NF-κB dimers and IκBα is similar and that the relative amounts of various NF-κB dimers and their affinities for IκBα are the determinants of their cytoplasmic retention.

EXPERIMENTAL PROCEDURES

Protein Expression and Purification—The cloning, expression, and purification of the NF-κB subunits and amino-terminal deletion mutants has been described previously (4, 6, 8, 9). The purification of p50dd/p65ddNLS, the p50RHR/p65RHR heterodimer, and its derivatives was accomplished by unfolding and refolding of purified components (9). In a second method, p50 and p65 have been coexpressed in *Escherichia coli* and purified as heterodimers. The full-length IκBα (residues 1–317) and IκBαΔSRD (residues 67–317) proteins were expressed as glutathione *S*-transferase (GST) fusion proteins in a pGEX vector (Novagen). They were both purified in a similar manner. The clone was transformed into BL21[DE3] cells and induced with 0.1 mM isopropylthio-β-D-galactoside overnight at room temperature. After cell lysis by sonication, the crude lysate was loaded onto a reduced glutathione-Sepharose column, followed by a Q Sepharose column and finally a Superdex75 gel filtration column (Amersham Pharmacia Biotech). The peak fractions were collected and stored at −80 °C. Untagged IκBαΔSRD (residues 67–317) and IκBαΔSRDΔPEST (residues 67–277) were cloned into a pET3a vector (Novagen) and purified as the GST-fusion proteins with the exception that the glutathione-Sepharose step was ignored.

DNA Purification—A 39-bp fluorescein labeled DNA was purchased from Yale University oligonucleotide synthesis facility. The DNA had the following sequence: 5′-fluorescein-GATCGCTG**GGGACTTTC-C**AGGGAGGCGTGGCCTGAGTCC-3′. The HIV-κB target site is shown in boldface. The complementary strand was synthesized on a Cyclone Plus DNA synthesizer. After deblocking, the oligonucleotides were purified over a Q-Sepharose column. Peak fractions were pooled and concentrated. Equimolar concentrations of the sense and antisense strands were mixed and annealed.

BIAcore Experiments—The BIAcore biosensor system allows the monitoring of macromolecular reactions in real time (32). The BIAcore system, sensor chips CM5 (certified), the amine coupling kit, and the anti-GST binding kit were obtained from BIAcore, Inc. The buffer used for all experiments was 10 mM HEPES (pH7.4), 150 mM NaCl, 3.4 mM EDTA, and 0.005% (v/v) Surfactant P20. To immobilize IκBα, an anti-GST antibody was first immobilized on the chip surface via amine coupling using the kit provided by the sensor chip manufacturer. Next, GST-IκBα was injected across the surface, and approximately 350 response units were captured onto the surface by the antibody per binding experiment. Two GST-IκBα constructs were tested with similar results: GST-IκBαΔSRD and GST-IκBα. Various rel/NF-κB constructs were then injected across the chip surface, and binding was monitored. At the end of each run, the GST-IκBα and NF-κB were removed from the surface with 10 μl of 10 mM glycine at pH 2.2, leaving active antibody on the surface. Each surface was used multiple times. To detect nonspecific binding to the GST and the immobilized antibody, control runs were performed with only antibody on the chip surface and with GST immobilized via the antibody on the surface. No significant nonspecific binding was observed. All experiments were performed at 25 °C and at a flow rate of 40 μl/min. All sensorgrams reported have been blank subtracted for any bulk refractive index effects.

Fluorescence Polarization—All fluorescence polarization measurements were made using the Beacon 2000 Fluorescence Polarization System (PanVera Corp.). We used fluorescence polarization to determine the DNA binding affinities of several NF-κB dimers (33). Serial dilutions of NF-κB were added to constant amounts of labeled DNA. The fluorescence polarization values were recorded once the system had reached equilibrium (approximately 50 min). All measurements were taken at 37 °C in 10 mM Tris (pH 7.5) and 50 mM NaCl. The fractional occupancy was calculated as described in Equation 1. K_D was calculated as the concentration of NF-κB at 0.5 fractional occupancy, as follows,

$$\text{Fractional occupancy} = (P - P_D)/(P_{ND} - P_D) \qquad \text{(Eq. 1)}$$

where P is polarization in millipolarization units, P_D is polarization of free DNA, and P_{ND} is polarization of DNA saturated with NF-κB.

Fluorescence Polarization Competition Assay—In the presence of IκBα and DNA, NF-κB links two competing equilibrium processes (see Equation 2). If the dissociation constant of one process is known, the dissociation constant of the second process can be derived from a competition assay. This assay probes the shift in equilibrium of one reaction when in the presence of a competing inhibitor. Having characterized the affinity of NF-κB for a particular κB-DNA target site, we endeavored to determine its affinity for IκBα binding by a fluorescence polarization competition assay. To perform this competition assay, varying concentrations of IκBα were mixed with constant amounts of NF-κB and labeled DNA. The system was allowed to reach equilibrium (approximately 1 h). We observed an increase in polarization with increased IκBα concentration. This corresponds to the generation of free DNA in solution upon the addition of IκBα to the preformed NF-κB/DNA complexes. Control experiments were performed to check for any nonspecific DNA binding by IκBα. IκBα does not bind DNA even at extremely high concentrations (50 μM). The competition assay binding curves were analyzed for IC_{50} values the concentration of IκBα at 0.5 fractional occupancy. The K_I value (the dissociation constant for the NF-κB/IκBα interaction) was derived using the following values according to Equation 5: the DNA binding affinity of NF-κB (K_D), the IC_{50} value, $[\text{NF-}\kappa\text{B}]_{total}$, and $[\text{DNA}]_{total}$, as follows,

$$\begin{array}{ccc} \text{NF-}\kappa\text{B} + \text{DNA} & \xrightleftharpoons{K_D} & \text{NF-}\kappa\text{B/DNA} \\ + & & \\ \text{I}\kappa\text{B} & & \\ K_I \Updownarrow & K_D = \dfrac{[\text{NF-}\kappa\text{B}][\text{DNA}]}{[\text{NF-}\kappa\text{B/DNA}]} & \dfrac{P_D - P}{P - P_{ND}} = \dfrac{[\text{NF-}\kappa\text{B/DNA}]}{[\text{DNA}]} \\ \text{NF-}\kappa\text{B/I}\kappa\text{B} & K_I = \dfrac{[\text{NF-}\kappa\text{B}][\text{I}\kappa\text{B}]}{[\text{NF-}\kappa\text{B/I}\kappa\text{B}]} & \end{array} \qquad \text{(Eq. 2)}$$

where $[\text{NF-}\kappa\text{B}]_{total} = [\text{NF-}\kappa\text{B}] + [\text{NF-}\kappa\text{B/I}\kappa\text{B}] + [\text{NF-}\kappa\text{B/DNA}]$, $[\text{DNA}]_{total} = [\text{DNA}] + [\text{NF-}\kappa\text{B/DNA}]$, and $[\text{I}\kappa\text{B}]_{total} = [\text{I}\kappa\text{B}] + [\text{NF-}\kappa\text{B/I}\kappa\text{B}]$. Solving for $[\text{NF-}\kappa\text{B}]_{total}$ in terms of $[\text{NF-}\kappa\text{B}]$, $[\text{I}\kappa\text{B}]_{total}$, $[\text{DNA}]$, K_D, and K_I yields the following expression,

$$[\text{NF-}\kappa\text{B}]_{total} = \frac{[\text{NF-}\kappa\text{B}]\{(K_I + [\text{NF-}\kappa\text{B}])(K_D + [\text{NF-}\kappa\text{B}]) + [\text{I}\kappa\text{B}]_{total}(K_D + [\text{NF-}\kappa\text{B}] + [\text{DNA}]_{total}(K_I + [\text{NF-}\kappa\text{B}])\}}{(K_I + [\text{NF-}\kappa\text{B}])(K_D + [\text{NF-}\kappa\text{B}])} \qquad \text{(Eq. 3)}$$

At the midpoint of the titration,

$$[\text{NF-}\kappa\text{B}] = K_D \text{ and } \frac{P_D - P}{P - P_{ND}} = 1 \quad \text{(Eq. 4)}$$

if $[\text{DNA}]_{\text{total}}$ and $[\text{NF-}\kappa\text{B}]_{\text{total}}$ are constant and [IκB] is varied. Then, at the IC_{50} of the competition binding curve, the following holds true.

$$K_I = \frac{-2\,K_D^2 - 2\,K_D IC_{50} - [\text{DNA}]_{\text{total}}\,K_D + 2\,K_D[\text{NF-}\kappa\text{B}]_{\text{total}}}{2\,K_D + [\text{DNA}]_{\text{total}} - 2[\text{NF-}\kappa\text{B}]_{\text{total}}} \quad \text{(Eq. 5)}$$

For each NF-κB dimer, the K_I values were calculated as an average of three individual experiments. Various ratios of [NF-κB]/[DNA] were tested, with similar results. There was less than a 20% error between individual experiments. All runs were performed in 10 mM Tris (pH 7.5) and 50 mM NaCl at 37 °C.

Native Polyacrylamide Gel Electrophoresis—10% native polyacrylamide gels were prepared in 0.25× Tris borate EDTA. The gels were filtered and degassed. Individual or complexed proteins were prepared in 10 mM Tris (pH 7.5), 4% glycerol, 2 mM β-mercaptoethanol, and 50 mM NaCl. Reactions were allowed to reach equilibrium at room temperature for 1 h. Native gel loading buffer (50 mM Tris, pH 7.5, 0.1% bromphenol blue, 10% glycerol, and 1.25 mM β-mercaptoethanol) was then added to each sample. The gels were run in 0.25× Tris borate EDTA for 1.5 h at 3 mA.

RESULTS

Protein Expression, Purification, and Experimental Design—To evaluate the contributions of the three segments within the RHR of NF-κB in complex formation with IκBα, a series of structure-based deletion mutants of the homodimers and of the heterodimer were prepared. Care was taken to ensure that the integrity of the three-dimensional fold of these mutants would remain intact. The flexible activation domain of p65, which follows the NLS, has been shown not to participate in the interaction with IκBα (3) and was therefore not included in this study. A list of the constructs pertinent to our studies is shown in Fig. 1, *A* and *B*. All proteins have been expressed in *E. coli* and purified to near homogeneity, as shown in Fig. 1*C*.

Interaction of IκBα with NFκB p50/p65 Heterodimer—We first determined the affinity of the wild type heterodimer (p50RHR/p65RHR) for the HIV-κB DNA using 0.1 nM labeled DNA and increasing amounts of the heterodimer. From the saturation binding curve, the equilibrium dissociation constant (K_D) of the NF-κB p50/p65-κB DNA complex was observed as 4.7 nM (Fig. 2*A*). We then performed a competition assay using the wild type p50RHR/p65RHR and IκBαΔSRD (IκBα with the amino-terminal signal response domain removed). These experiments show that IκBα binds the wild type heterodimer with an equilibrium dissociation constant (K_I) of 3.0 nM (Fig. 2*A*). In an effort to determine the contribution of the SRD of IκBα, we repeated the fluorescence polarization competition experiment using the full-length IκBα and IκBαΔSRD as glutathione *S*-transferase fusion proteins (GST-IκBα and GST-IκBαΔSRD). The inhibition curves resulting from the full-length GST-IκBα, GST-IκBαΔSRD, and IκBαΔSRD are nearly identical (Fig. 2*B*). Further controls confirmed that GST does not interact nonspecifically with the NF-κB or the labeled DNA (data not shown). These results confirm that the SRD of IκBα does not contribute to binding of the NF-κB p50/p65 heterodimer. Therefore, we chose to use IκBαΔSRD in our assays for measuring the NF-κB/IκBα binding constants.

We next investigated the role of the carboxyl-terminal acidic tail/PEST sequence of IκBα in the inhibition of DNA binding by the p50/p65 heterodimer. We performed the fluorescence polarization competition experiment previously described using a mutant IκBα with both the SRD and PEST sequence removed (IκBαΔSRDΔPEST). Even at a 150-fold excess of IκBαΔSRDΔPEST, only a slight decrease in the polarization was observed (Fig. 2*B*). This result identifies the acidic tail/PEST sequence as the necessary element that confers DNA-inhibitory binding activity on IκBα.

TABLE I
K_I and ΔG values calculated from the fluorescence polarization competition assays

Each K_I value reported is an average of three individual experiments. The K_I values were calculated using the equations discussed under "Experimental Procedures." The K_D values (the DNA binding constants) of the various homo- and heterodimers were determined independently.

Dimer	K_I	ΔG
	nM	*kcal/mol*
p50RHR/p65RHR	3.0 ± 0.7	−11.6
p50RHRs/p65RHR	3.1 ± 0.7	−11.6
p50RHR/p65RHRs	16.9 ± 1.3	−10.6
p50RHRs/p65RHRs	28.0 ± 2.3	−10.3
p50RHR/p65RHR(ΔL1)	172.7 ± 25.9	−9.2
p65RHR/p65RHR	82.1 ± 14.0	−9.7
p65RHRs/p65RHRs	143.3 ± 11.2	−9.3
p50RHR/p50RHR	181.3 ± 16.4	−9.2
p50RHRs/p50RHRs	1518.3 ± 110.4	−7.92

The Role of the NLSs of the Heterodimer in Contacting IκBα—It is well understood that the nuclear localization of NF-κB dimers is mediated by the nuclear localization signals located at the carboxyl termini of the RHR. However, the exact mode of NLS masking by IκBα remains unclear. To delineate the role of NLSs of the NF-κB heterodimer, we have made three heterodimer variants in which the NLS is individually and doubly removed (p50RHR/p65RHRs, p50RHRs/p65RHR, and p50RHRs/p65RHRs,where *s* refers to the shortened RHR, with its NLS removed). As seen in Fig. 3*A*, the mutant heterodimer with deleted p65 NLS (p50RHR/p65RHRs) has over 5-fold lower affinity for IκBα compared with that of the wild type heterodimer ($K_I \sim 16.9$ nM p50RHR/p65RHRs *versus* 3.0 nM p50RHR/p65RHR). On the other hand, p50RHRs/p65RHR binds IκBα with an affinity of 3.1 nM. When both the NLSs are removed, the heterodimer shows a 9-fold ($K_I \sim 28.0$ nM) defect compared with the wild type heterodimer (Table I). Clearly, the p65NLS is essential for IκBα binding. The role of the p50 NLS is not apparent from the p50RHRs/p65RHR binding profile, which looks similar to the wild type heterodimer. However, if the NLS of p50 was not involved in any contact with IκBα, we would expect the p50RHR/p65RHRs and the p50RHRs/p65RHRs binding profiles to be identical. The 1.6-fold defect in p50RHRs/p65RHRs binding affinity when compared with p50RHR/p65RHRs indicates that the p50NLS does in fact contribute to IκBα binding. Therefore, both the NLSs of p50 and p65 appear to be involved in direct interactions with IκBα. These results establish, for the first time, a specific role for the p50 subunit of the heterodimer in IκBα binding specificity. The p50 subunit is not, it seems, simply an inert participant in the complex formation by nature of its ability to dimerize with the p65 subunit.

In support of our results obtained from the fluorescence polarization competition assay, we have performed biomolecular interaction assays on wild type and shortened NF-κB proteins using BIAcore technology. The sensorgram shown in Fig. 3*B* provides two important points: first, the nature of the interaction between the wild type heterodimer and IκBα is complex, and both the association and dissociation are multiphasic; and second, the p50RHRs/p65RHRs heterodimer is defective for IκBα binding when compared with the wild type heterodimer. The role of the p50NLS was further probed by using two truncated heterodimeric p50/p65 constructs, in which the amino-terminal domain of the p50 subunit was deleted (p50ddNLS/p65RHR and p50dd/p65RHR). As seen in Fig. 3*C*, when the NLS of the p50 subunit is deleted (p50dd/p65RHR), the heterodimer becomes a poorer substrate for IκBα compared

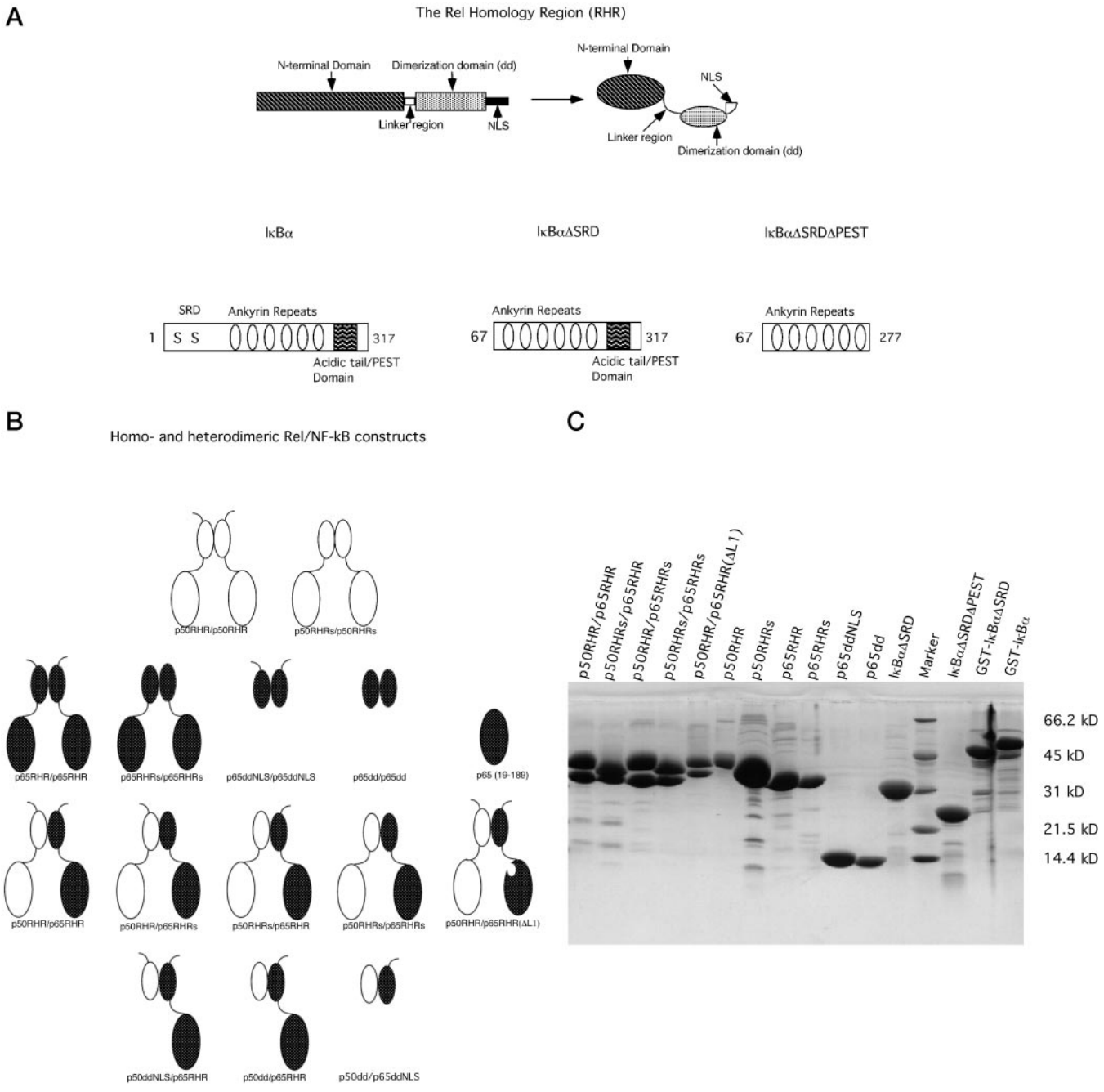

FIG. 1. *A, top*, on the *left,* shown schematically, is the linear representation of the RHR depicting the amino-terminal domain, the dimerization domain, and the NLS. On the *right*, shown schematically, is the folded structure of the RHR as revealed by the its three-dimensional structure. *Bottom*, the full-length IκBα and truncated IκBα, (IκBαΔSRD, and IκBαΔSRDΔPEST) are shown schematically. Serines 32 and 36 are indicated in the SRD domain of full-length IκBα. The ankyrin repeats are shown by the *ovals,* and the acidic tail/PEST sequence is shown with a *box*. *B*, schematic representation of the various homo- and heterodimeric NF-κB RHR dimers and their mutational variants. The p50RHR/p65RHRΔL1 is a deletion of residues 30–45 in the p65 subunit shown by a *small open circle* within the p65RHR. *C*, 15% SDS-polyacrylamide gel electrophoresis of purified NF-κB and IκBα proteins. In each lane, at least 10 μg of protein was loaded.

with the one with the NLS. Again, this result underscores the importance of the p50 NLS in IκBα binding.

The DNA Binding Loop L1 of the p65 Subunit of the p50/p65 Heterodimer Is Involved in IκBα Recognition—The involvement of the acidic tail of IκBα in the inhibition of DNA binding activity of NF-κB led researchers to speculate that the amino-terminal DNA binding domain of NF-κB is involved in contacting IκBα (30, 34–36). Kumar and Gelinas (36) found that a small peptide homologous to the v-Rel amino-terminal DNA binding domain competed with the full-length v-Rel for IκBα binding. In order to investigate whether the amino-terminal DNA binding domain of p65 may be involved in interacting with IκBα, we constructed an NF-κB p50/p65 heterodimer in which a segment of 15 amino acids (residues 30–45 of p65) has been replaced by three glycine residues at loop L1 of p65. Four of the five residues that mediate direct DNA base-specific contacts, Arg^{33}, Arg^{35}, Tyr^{36}, and Glu^{39} are located within this 15-amino acid segment. As expected, the mutant heterodimer binds to HIV-κB DNA with reduced affinity (237.8 nM). However, this affinity is high enough to perform the fluorescence polarization competition assay with IκBα. We were able to determine that IκBα binds to this mutant heterodimer with a

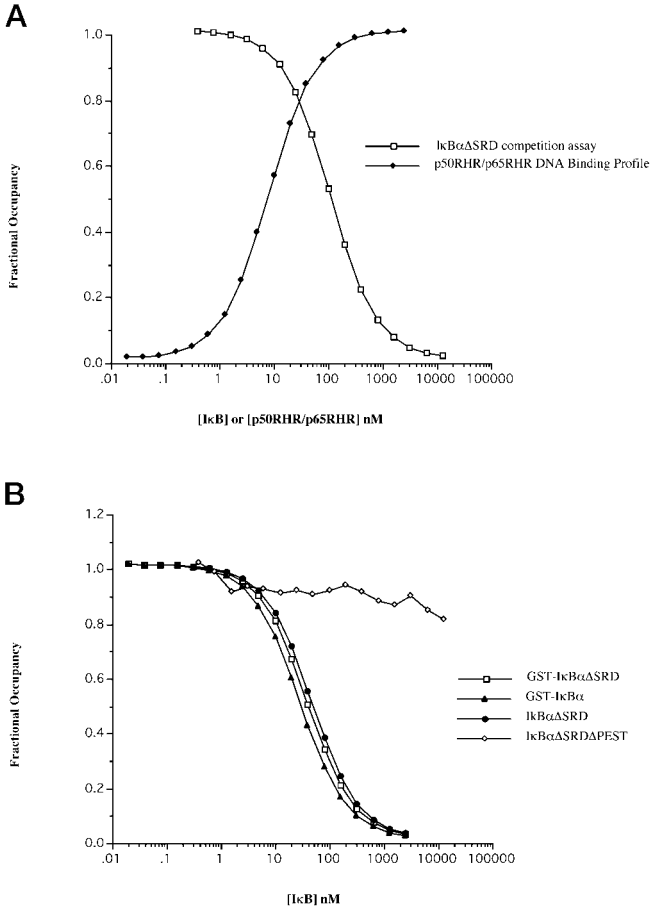

FIG. 2. *A*, overlay of the p50RHR/p65RHR DNA binding curve (*filled diamonds*) with the IκBαΔSRD/p50RHR/p65RHR/DNA competition assay (*open squares*). In the DNA binding assay, 0.1 nM labeled DNA was used with varying concentrations of p50RHR/p65RHR (0.015 nM to 2 μM). In the competition assay, 60 nM p50RHR/p65RHR and 6 nM labeled DNA were used with varying amounts of IκBαΔSRD (0.3 nM to 10 μM). *B*, overlay of GST-IκBαΔSRD, GST-IκBα, IκBαΔSRD, and IκBαΔSRDΔPEST proteins in a competition assay with 25 nM p50RHR/p65RHR and 2.5 nM DNA.

K_I of 172.7 nM (Table I). This indicates a 57-fold reduction in binding affinity compared with the wild type heterodimer, showing that the amino-terminal domain of the p65 subunit is involved in contacting IκBα.

Interaction of the p65 Homodimer with IκBα—In vivo transfection followed by immunoprecipitation and qualitative DNA binding inhibition using a gel retardation assay showed that p65 homodimer can be retained in the cytoplasm by IκBα with high efficiency (25). Therefore, one of the objectives of this study was to determine whether the p65 homodimer has an affinity identical or comparable to that of the wild type heterodimer for IκBα. Results from fluorescence polarization competition assays (Fig. 4*A*) show that IκBα has roughly a 27-fold weaker affinity for p65RHR homodimer than the wild type heterodimer. We observed that removal of the p65 NLSs reduces its affinity for IκBα by more than 2-fold compared with the wild type p65 homodimer. These results indicate that the NLSs of the p65 homodimer and of the p50/p65 heterodimer contribute differentially toward the binding energy of the respective complexes. We have also tested whether the monomeric amino-terminal domain of p65RHR (residues 19–189, see Fig. 1*B*) retains any significant affinity to interact with IκBα. Because the DNA binding affinity of this fragment of p65 is very low (>1 μM), we used the surface plasmon resonance assay only to obtain this information. As shown in Fig. 4*B*, this

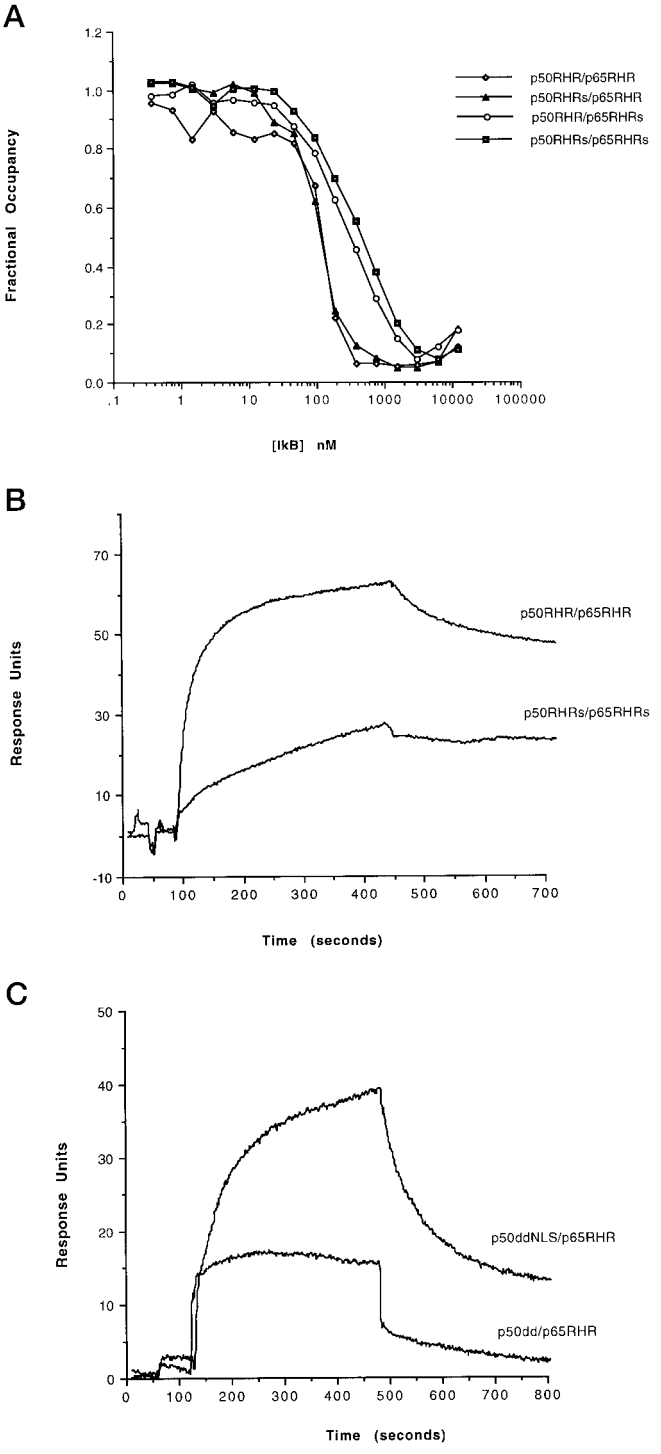

FIG. 3. *A*, fluorescence polarization competition assay with wild type, singly mutated, or doubly mutated NLS(s) of the p50RHR/p65RHR. All assays were performed with 60 nM NF-κB, 6 nM DNA, and varying concentrations of IκBαΔSRD (0.3 nM to 10 μM). Removal of the p50 or p65 NLS had no effect on the DNA binding. *B*, binding curves for p50RHR/p65RHR and p50RHRs/p65RHRs generated from BIAcore experiments. For each run, approximately 350 response units of GST-IκBαΔSRD were immobilized on the surface. 10 nM of each NF-κB protein was injected across the surface at a flow rate of 40 μl/min for a total of 6 min and allowed to dissociate from the surface for 10 min before regenerating with 10 mM glycine (pH 2.2). *C*, binding curves for p50ddNLS/p65RHR and p50dd/p65RHR generated from BIAcore experiments. 350 response units of GST-IκBαΔSRD were immobilized on the surface. 20 nM of each protein was injected across the surface at a flow rate of 40 μl/min for 6 min followed by a 10-min dissociation time.

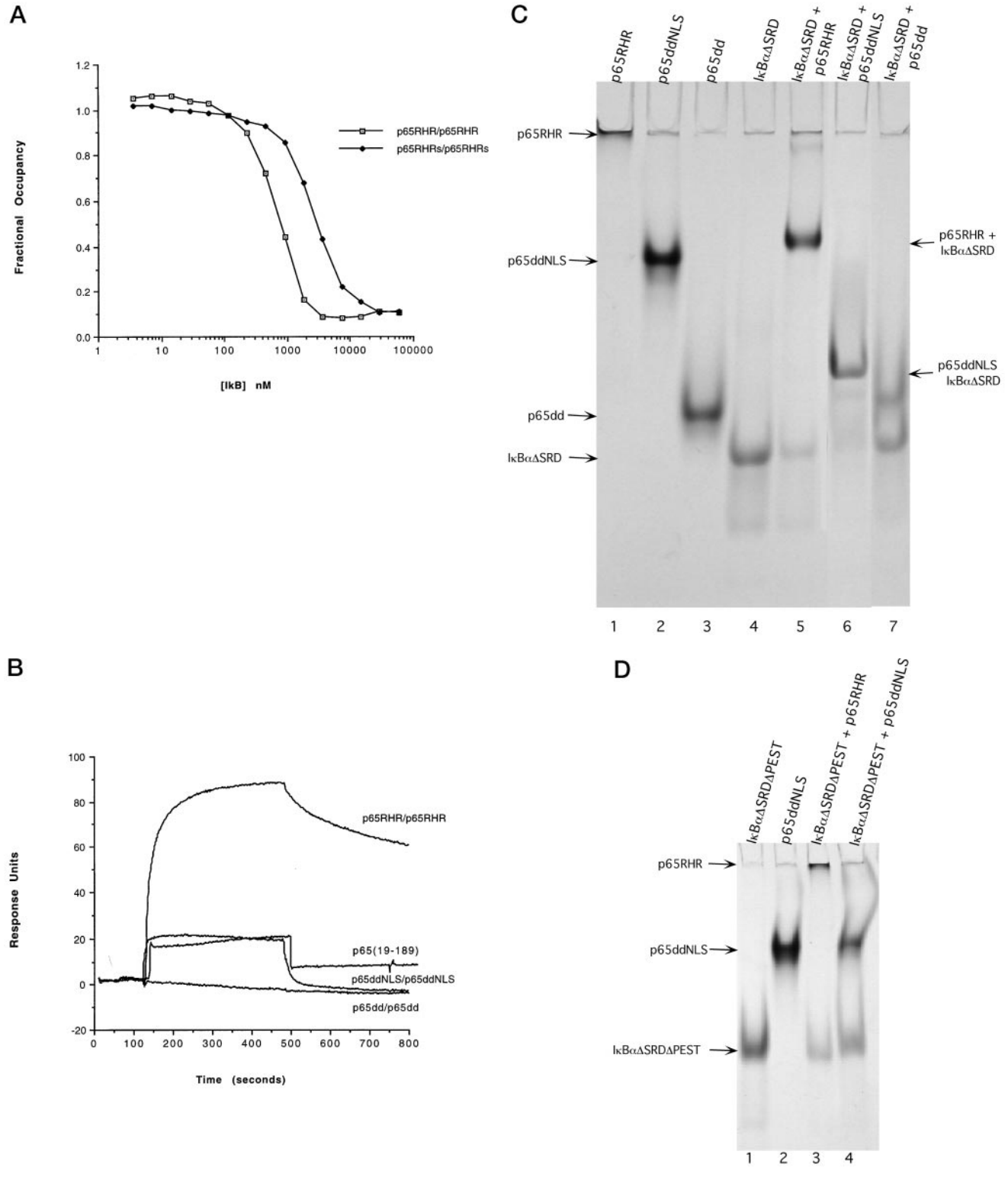

FIG. 4. *A*, fluorescence polarization competition assay for two p65RHR/p65RHR or p65RHRs/p65RHRs with IκBαΔSRD. For each binding curve 1 μM p65 and 10 nM of labeled DNA was used with varying concentrations of IκBαΔSRD. The DNA binding constant (K_D) for both p65RHR and p65RHRs homodimers was approximately 301.9 nM. *B*, overlay of binding curves for the wild type p65 homodimer (p65RHR), two mutational variants (p65ddNLS and p65dd), and the monomeric amino-terminal p65 (19–189) generated from BIAcore experiments. Approximately 350 response units of GST-IκBαΔSRD were immobilized on the surface for each experiment. 20 nM each protein was injected across the chip surface for 6 min at a flow rate of 40 μ/min, followed by a 10 min dissociation phase. *C*, 10% polyacrylamide native gel depicting the shift of individual and complexed p65 homodimers. 10 μg of total protein was loaded into each lane. Equimolar amounts of p65 homodimer and IκBαΔSRD were used in the complexes with buffer conditions as described under "Experimental Procedures." *Lane 1*, 30 μM p65RHR; *lane 2*, 30 μM p65ddNLS; *lane 3*, 30 μM p65dd; *lane 4*, 30 μM IκBαΔSRD; *lane 5*, 30 μM IκBαΔSRD and 30 μM p65RHR; *lane 6*, 30 μM IκBαΔSRD and 30 μM p65ddNLS; *lane 7*, 30 μM IκBαΔSRD and 30 μM p65dd. *D*, 10% polyacrylamide native gel depicting the interaction of the IκBαΔSRDΔPEST and the p65 homodimers. 10 μg of total protein was loaded into each lane. Equimolar amounts of IκBαΔSRDΔPEST and p65 were mixed in lanes with complexed proteins in 50 mM NaCl and buffer conditions as described under "Experimental Procedures." *Lane 1,* 30 μM IκBαΔSRDΔPEST; *lane 2*, 30 μM p65ddNLS; *lane 3*, 30 μM IκBαΔSRDΔPEST and 30 μM p65RHR; *lane 4*, 30 μM IκBαΔSRDΔPEST and 30 μM p65ddNLS.

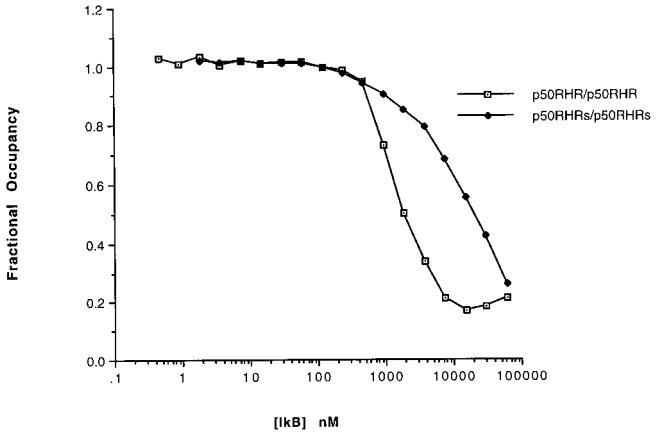

FIG. 5. **Fluorescence polarization competition assay for two p50RHR and p50RHRs homodimers.** For each binding curve, 500 nM p50 and 5 nM labeled DNA was used with varying concentrations of IκBαΔSRD. The DNA binding constant (K_D) for both homodimeric p50RHR and p50RHRs was approximately 52.2 nM.

domain of p65 displays negligible affinity for IκBα. In comparison, the sensorgram of the p65RHR clearly indicates a strong interaction.

The p65 Homodimer with the Amino-terminal Domain Deleted Forms an Unstable Complex with IκBα—Our earlier results suggest that the amino-terminal domain of p65 in p50/p65 heterodimer is involved in IκBα recognition. To test whether the amino-terminal domain is also involved in the context of the p65 homodimer, we made two different constructs of the p65 homodimer. One construct lacks the amino-terminal domain of the RHR (p65ddNLS-for p65 dimerization domain containing NLS), and a second construct has both the amino-terminal domain and the short, 13-amino acid tail removed (p65dd). The proteins prepared from these constructs do not bind DNA with any specificity. Therefore, we could not use the fluorescence polarization competition assay to determine the precise affinities of these proteins for IκBα. However, we did observe complex formation between GST-IκBα and p65ddNLS using the BIAcore assay. As shown in Fig. 4*B*, the off rate of this interaction is fast. In contrast to the binding of p65ddNLS, the binding kinetics of the p65RHR/IκBα complex shows a much slower dissociation rate. The p65dd, on the other hand, shows very little binding, which confirms the important role of the NLSs of p65 in IκBα binding. In order to further characterize the role of the p65 NLS, we compared the binding affinity of p65ddNLS and p65dd for IκBα using native gel electrophoresis. As shown in Fig. 4*C*, p65ddNLS but not p65dd can bind to IκBα. However, the p65ddNLS complex, rather than exhibiting the compact stable protein complex band illustrated by the p65RHR/IκBα lanes, instead shows a diffuse band, indicative of an unstable complex. This result was observed despite the fact that the concentration of p65 and IκBα used was over 360-fold above the K_I of the complex. We have verified the activity of p65RHR and of p65ddNLS for their interaction with IκBαΔSRDΔPEST using gel mobility shift assay. As shown in Fig. 4*D*, no complex was observed between p65 homodimer and IκBαΔSRDΔPEST. Overall, these experiments allow us to draw the following conclusions: 1) the NLSs of p65RHR are important for IκBα binding; 2) in the absence of its amino-terminal domain, p65 forms an unstable complex with IκBα; and 3) the p65RHR and the p50/p65 heterodimer require similar segments of IκBα for complex formation.

Interaction of the p50 Homodimer with IκBα—It has been reported that IκBα is unable to inhibit the DNA binding activity of the p50 homodimer even though these proteins can associate with each other to form a complex (37). We tested whether our assay could detect and measure the inhibition of the p50 homodimer/DNA complex by IκBα. We were also interested in observing whether the overall mode of the interaction between IκBα and the p50 homodimer is similar to that of the other two complexes. As seen in Fig. 5, our fluorescence polarization competition assay illustrates that DNA binding by the p50 homodimer is inhibited by IκBα. However, IκBα is a much poorer inhibitor of p50 DNA binding when compared with its inhibitory activities toward the p50/p65 heterodimer or the homodimer of p65. The affinity of IκBα for the p50 homodimer is 50-fold weaker than the p50/p65 heterodimer and 2.2-fold weaker than the p65 homodimer (Table I). The affinity of IκBα for the p50RHRs, which is devoid of its NLSs, is further reduced by 8-fold, making this p50 homodimer 500-fold defective compared with the wild type p50/p65 heterodimer (Table I). This drastic decrease in affinity suggests that at least one of the NLSs and possibly both the NLSs of the p50 homodimer are involved in contacting IκBα. These observations also demonstrate that the NLSs of p50 play a more dominant role in IκBα binding than the NLSs of the p65 homodimer.

DISCUSSION

The NLSs of NF-κB Are Engaged in Interactions with IκBα—The NF-κB NLSs have been shown to be responsible for nuclear translocation, yet, how IκBα blocks these sequences to retain the NF-κB dimers in the cytoplasm has remained unclear. Studies that showed that these sequences are not required for interactions with IκBα suggested a steric exclusion of the NLSs upon complexation with IκBα (38, 39). Other studies showed that IκBα directly interacts with the NLS (29, 40–43). Our experiments demonstrate that the NLSs of the NF-κB dimers are required to bind IκBα with maximum affinity. This observation presents two possible roles for the NLSs upon NF-κB/IκBα complex formation: 1) the NLSs make direct contacts with IκBα; or 2) the NLSs play a more indirect role by altering the conformation of the complex to enhance binding. We believe that because the NLSs are not part of the folded structures of the RHR of p50 and p65, these sequences (NLSs) are not capable of altering the conformation of the complex without making direct contacts with IκBα. Therefore, we argue that the carboxyl-terminal 13-amino acid segments of both p50 and p65 RHR, although flexible in solution, adopt a new stable conformation by mediating direct contacts with IκBα. Our results also indicate that the contributions of the NLSs in the binding energy of the complex differ for the various NF-κB dimers. Although each NLS of the heterodimer plays only a modest role individually in contacting IκBα, together they make a significant contribution to the affinity of the interaction. The differential contribution of the NLSs to complex formation could be due two reasons. First, the amino acid sequences of the carboxyl-terminal 13-residue segments differ significantly in p50 and p65, suggesting that the nature of contacts formed by these sequences with IκBα are different. Second, each of the three dimers presents a unique dimerization domain platform upon which IκBα binds. It can be imagined that upon association, the dimerization domain binding platform of NF-κB might induce slightly different conformational changes on IκBα. These variations may then direct the NLSs to encounter different surfaces of IκBα.

Inhibition of NF-κB-DNA Binding by IκBα—Arenzana-Seisdedos *et al.* (31) have shown that post-induction newly synthesized IκBα can enter the nucleus, where it is able to remove NF-κB from its DNA binding site and return it to the cytoplasm. Our study demonstrates that the DNA binding loop L1 of p65RHR plays a critical role in IκBα binding. A reduction of more than 2 kcal/mole of binding free energy results from the deletion of a part of this loop. This suggests a loss of multiple

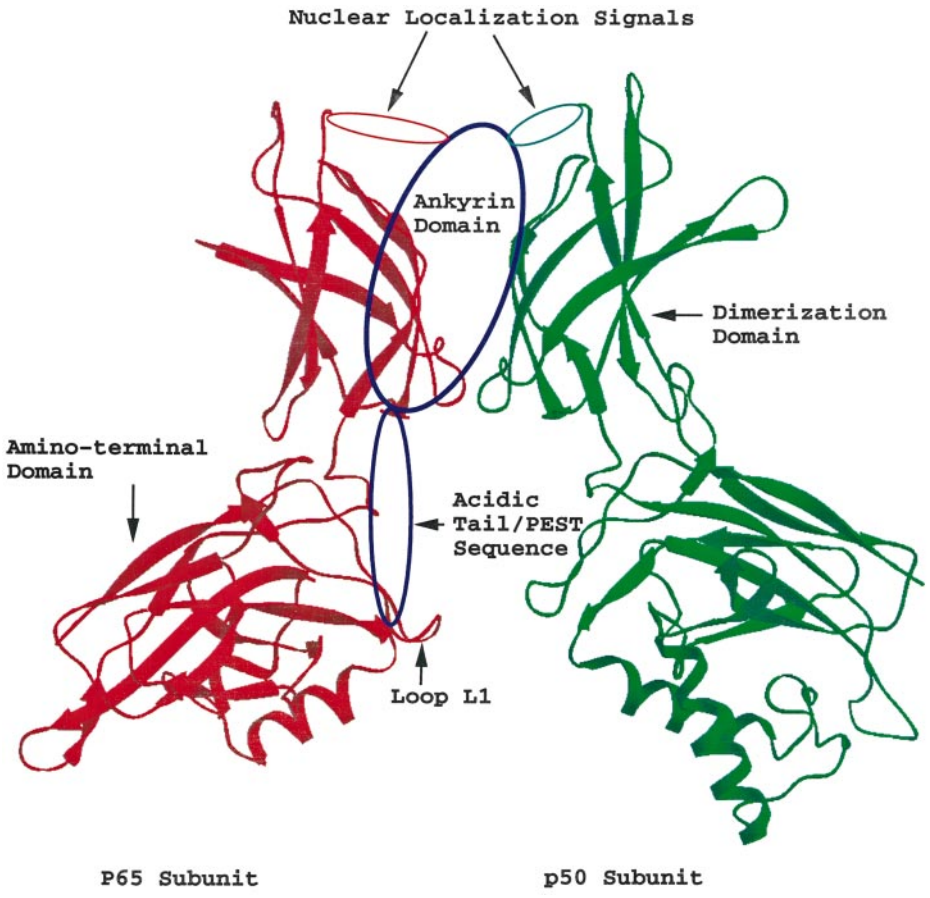

FIG. 6. **A tentative model of the NF-κB p50/p65/IκBα complex is shown schematically.** The IκBαΔSRD is shown in *blue ovals*. The crystallographic model of NF-κB (p50/p65) is presented as a ribbon drawing. The p50 and p65 NLSs are not part of the true crystallographic model.

direct contacts between IκBα and NF-κB likely to be mediated by these residues. The removal of both the amino-terminal domains in p50 and p65 homodimers renders them poor partners for interactions with IκBα. In a reciprocal fashion, we have also shown that the removal of the acidic tail/PEST sequence of IκBα converts it to a poor inhibitor of the NF-κB/DNA complex. Taken together, these results imply that the acidic tail of IκBα is responsible, at least in part, for contacting the amino-terminal domain. It is possible that these contacts are mainly nonspecific and electrostatic in nature. That the p65 loop L1 of the p50/p65 heterodimer is involved in contacting the acidic tail of IκBα is mainly due to the close proximity of the p65 loop L1 and the acidic tail of IκBα. In the case of the p50 homodimer/IκBα complex, we believe that one of the L1 loops is involved in a type of contact similar to that of the p65 loop L1 in the p65 homodimer and in the p50/p65 heterodimer. The interactions between the DNA recognition element of the NF-κB dimers and the acidic tail of IκBα might be analogous to the nonspecific DNA phosphate contacts by basic amino acids. Several serines and threonines of the carboxyl-terminal acidic tail/PEST sequence of IκBα are known to be phosphorylated by casein kinase II (45–47). The carboxyl-terminal phosphorylated IκBα may exhibit a much higher affinity for the NF-κB dimers. Additional ion pairing interactions between the negatively charged phosphates and other basic residues may explain why this modified form of IκBα is a more potent dissociator of NF-κB/DNA complexes than the unmodified IκBα (30).

A Model of the Complex—Our understanding of the crystal structures of the p50 and p65 homodimers and the p50/p65 heterodimer suggests that the monomeric subunits of these dimers are composed of three segments, each capable of independent motion. Although a crystal structure of IκBα is not available, the structural similarity of three distantly related ankyrin repeat-containing proteins suggests that the ankyrin domain of IκBα and of other IκB family proteins might assume a similar folded structure. This is further supported by our preliminary circular dichroism data, which show that IκBα is primarily α-helical (data not shown). It appears that the carboxyl-terminal acidic tail/PEST sequence of IκBα is a flexible unit independent of the ankyrin domain. The fact that all five segments extending from the interacting proteins participate in direct contacts upon complex formation complicates the reaction binding kinetics. It has been speculated that IκB-related proteins occupy the groove located on the top of the dimerization domain. An indirect conformational alteration of the NF-κB proteins upon binding to IκB was proposed as the mechanism of inhibition of DNA binding by the Rel proteins (1, 2). This idea was supported by two genetically isolated mutants of Dorsal, which are defective in binding Cactus, the *D. melanogaster* IκB homologue. The two mutations were mapped to the groove formed between the Dorsal dimerization domain (48). We have used the structures of other ankyrin repeat proteins coupled with biochemical information about complex formation to develop a preliminary structural model of this interaction. Based on the crystal structure of 53BP2, an ankyrin repeat-containing inhibitor of DNA binding by p53, one can estimate that the linear distance occupied by the one face of six ankyrin repeats of IκBα is roughly 40 Å. This distance is approximately the diagonal distance of the β-sheet platform formed by the dimer. We speculate that the ankyrin repeat domain of IκBα sits diagonally across the β-sheet platform formed by the dimerization domains of both NF-κB subunits (as seen in Fig. 6). In this orientation the carboxyl-terminal acidic tail/PEST sequence can interact with the basic DNA binding residues of p65. This model predicts that the amino-terminal ankyrin repeats make contacts primarily with the p50 portion of the

dimerization domain, whereas the carboxyl-terminal portion of the ankyrin repeat domain is engaged with the p65 subunit. Our model explains how IκBα can directly contact both the NLSs and the DNA binding loop L1 of p65 and still interact with the homologous Dorsal mutation sites.

Biological Significance—Tissue specific and signal dependent expression of NF-κB and IκB proteins reveal a complex profile of the nucleo-cytoplasmic distribution of the NF-κB/IκB complexes in a given cell type (3, 12). Furthermore, differential dimerization propensities between the NF-κB proteins provide an additional level of complexity. Without proper knowledge of all these parameters, a true picture of NF-κB regulation cannot be depicted. However, the current knowledge identifies the existence of p50 homodimer in the nucleus, whereas the p50/p65 heterodimer remains in the cytoplasm in complex with IκBα (also with IκBβ) in the resting cell. This information suggests that the p50 homodimer is expressed at a high level yet escapes the cytoplasmic inhibition by IκBα (3). We propose that the significantly lower affinity of the p50/IκBα complex compared with the p50/p65/IκBα complex explains the differential distribution of the dimers. Lower concentrations of the p65 homodimer in most cells explain why this homodimer is not usually detected the cytoplasm. We propose that the cytoplasmic/nuclear partitioning of the NF-κB dimers is delicately balanced by the concentrations of these proteins and their relative affinities for IκB family proteins, in addition to the other factors mentioned above.

Acknowledgments—We thank Dr. S. Taylor for making the BIAcore available for our use and S. Demer for assistance with the BIAcore experiments. We are grateful to Dr. J. Kyte for help with the competition assay. We acknowledge Drs. P. Jennings, P. Ghosh, and G. Van Duyne for reading the manuscript. We thank Dr. De-Bin Huang for Fig. 6 and the other members of our laboratory for critically reading the manuscript.

REFERENCES

1. Baeuerle, P. A., and Henkel, T. (1994) *Annu. Rev. Immunol.* **12,** 141–179
2. Siebenlist, U., Franzoso, G., and Brown, K. (1994) *Annu. Rev. Cell Biol.* **10,** 405–455
3. Baldwin, A. S., Jr. (1996) *Annu. Rev. Immunol.* **14,** 649–683
4. Ghosh, G., van Duyne, G., Ghosh, S., and Sigler, P. B. (1995) *Nature* **373,** 303–310
5. Muller, C. W., Rey, F. A., Sodeoka, M., Verdine, G. L., and Harrison, S. C. (1995) *Nature* **373,** 311–317
6. Huang, D.-B., Huxford, T., Chen, Y.-Q., and Ghosh, G. (1997) *Structure* **5,** 1427–1436
7. Cramer, P., Larson, C. J., Verdine, G. L., and Muller, C. W. (1997) *EMBO J.* **16,** 7078–7090
8. Chen, Y. Q., Ghosh, S., and Ghosh, G. (1998) *Nat. Struct. Biol.* **5,** 67–73
9. Chen, F. E., Huang, D. B., Chen, Y. Q., and Ghosh, G. (1998) *Nature* **391,** 410–413
10. Traenckner, E. B., Pahl, H. L., Henkel, T., Schmidt, K. N., Wilk, S., and Baeuerle, P. A. (1995) *EMBO J.* **14,** 2876–2883
11. Brown, K., Franzoso, G., Baldi, L., Carlson, L., Mills, L., Lin, Y. C., Gerstberger, S., and Siebenlist, U. (1997) *Mol. Cell. Biol.* **17,** 3021–3027
12. Verma, I. M., Stevenson, J. K., Schwarz, E. M., Van Antwerp, D., and Miyamoto, S. (1995) *Genes Dev.* **9,** 2723–2735
13. Chen, Z., Hagler, J., Palombella, V. J., Melandri, F., Scherer, D., Ballard, D., and Maniatis, T. (1995) *Genes Dev.* **9,** 1586–1597
14. Geisler, R., Bergmann, A., Hiromi, Y., and Nusslein-Volhard, C. (1992) *Cell* **71,** 613–621
15. Kidd, S. (1992) *Cell* **71,** 623–635
16. Steward, R. (1987) *Science* **238,** 692–694
17. Gorina, S., and Pavletich, N. P. (1996) *Science* **274,** 1001–1005
18. Luh, F. Y., Archer, S. J., Domaille, P. J., Smith, B. O., Owen, D., Brotherton, D. H., Raine, A. R., Xu, X., Brizuela, L., Brenner, S. L., and Laue, E. D. (1997) *Nature* **389,** 999–1002
19. Venkataramani, R., Swaminathan, K., and Marmorstein, R. (1998) *Nat. Struct. Biol.* **5,** 74–81
20. Batchelor, A. H., Piper, D. E., de la Brousse, F. C., McKnight, S. L., and Wolberger, C. (1998) *Science* **279,** 1037–1041
21. Jaffray, E., Wood, K. M., and Hay, R. T. (1995) *Mol. Cell. Biol.* **15,** 2166–2172
22. Whiteside, S. T., Ernst, M. K., LeBail, O., Laurent-Winter, C., Rice, N., and Israel, A. (1995) *Mol. Cell. Biol.* **15,** 5339–5345
23. Brockman, J. A., Scherer, D. C., McKinsey, T. A., Hall, S. M., Qi, X., Lee, W. Y., and Ballard, D. W. (1995) *Mol. Cell. Biol.* **15,** 2809–2818
24. Rogers, S., Wells, R., and Rechsteiner, M. (1986) *Science* **234,** 364–368
25. Ernst, M. K., Dunn, L. L., and Rice, N. R. (1995) *Mol. Cell. Biol.* **15,** 872–882
26. Leveillard, T., and Verma, I. M. (1993) *Gene Expr.* **3,** 135–150
27. Naumann, M., Wulczyn, F. G., and Scheidereit, C. (1993) *EMBO J.* **12,** 213–222
28. Baeuerle, P. A., and Baltimore, D. (1996) *Cell* **87,** 13–20
29. Beg, A. A., Ruben, S. M., Scheinman, R. I., Haskill, S., Rosen, C. A., and Baldwin, A. S., Jr. (1992) *Genes Dev.* **6,** 1899–1913
30. Tran, K., Merika, M., and Thanos, D. (1997) *Mol. Cell. Biol.* **17,** 5386–5399
31. Arenzana-Seisdedos, F., Thompson, J., Rodriguez, M. S., Bachelerie, F., Thomas, D., and Hay, R. T. (1995) *Mol. Cell. Biol.* **15,** 2689–2696
32. Jonsson, U., Fagerstam, L., Lofas, S., Stenberg, E., Karlsson, R., Frostell, A., Markey, F., and Schindler, F. (1993) *Ann. Biol. Clin.* **51,** 19–26
33. LeTilly, V., and Royer, C. A. (1993) *Biochemistry* **32,** 7753–7758
34. Diehl, J. A., McKinsey, T. A., and Hannink, M. (1993) *Mol. Cell. Biol.* **13,** 1769–1778
35. Kerr, L. D., Inoue, J., Davis, N., Link, E., Baeuerle, P. A., Bose, H. R., Jr., and Verma, I. M. (1991) *Genes Dev.* **5,** 1464–1476
36. Kumar, S., and Gelinas, C. (1993) *Proc. Natl. Acad. Sci. U. S. A.* **90,** 8962–8966
37. Bell, S., Matthews, J. R., Jaffray, E., and Hay, R. T. (1996) *Mol. Cell. Biol.* **16,** 6477–6485
38. Govind, S., Drier, E., Huang, L. H., and Steward, R. (1996) *Mol. Cell. Biol.* **16,** 1103–1114
39. Rottjakob, E. M., Sachdev, S., Leanna, C. A., McKinsey, T. A., and Hannink, M. (1996) *J. Virol.* **70,** 3176–3188
40. Latimer, M., Ernst, M. K., Dunn, L. L., Drutskaya, M., and Rice, N. R. (1998) *Mol. Cell. Biol.* **18,** 2640–2649
41. Ganchi, P. A., Sun, S. C., Greene, W. C., and Ballard, D. W. (1992) *Mol. Biol. Cell* **3,** 1339–1352
42. Tatei, K., and Levine, M. (1995) *Mol. Cell. Biol.* **15,** 3627–3634
43. Luque, I., and Gelinas, C. (1998) *Mol. Cell. Biol.* **18,** 1213–1224
44. Deleted in proof
45. Lin, R., Beauparlant, P., Makris, C., Meloche, S., and Hiscott, J. (1996) *Mol. Cell. Biol.* **16,** 1401–1409
46. McElhinny, J. A., Trushin, S. A., Bren, G. D., Chester, N., and Paya, C. V. (1996) *Mol. Cell. Biol.* **16,** 899–906
47. Schwarz, E. M., Van Antwerp, D., and Verma, I. M. (1996) *Mol. Cell. Biol.* **16,** 3554–3559
48. Lehming, N., McGuire, S., Brickman, J. M., and Ptashne, M. (1995) *Proc. Natl. Acad. Sci. U. S. A.* **92,** 10242–10246